EUROPEAN ORGANIZATION FOR NUCLEAR RESEARCH
Laboratory for Particle Physics

# A CRYOGENIC HIGH-REYNOLDS TURBULENCE EXPERIMENT AT CERN

A. Bézaguet[1], J.-P. Dauvergne[1], S. Knoops[1], Ph. Lebrun[1], M. Pezzetti[1],
O. Pirotte[1], J.-L. Bret[2], B. Chabaud[2], G. Garde[2], C. Guttin[2], B. Hébral[2],
S. Pietropinto[2], P. Roche[2], J.-P. Barbier-Neyret[3], C. Baudet[3], Y. Gagne[3],
C. Poulain[3], B. Castaing[4], Y. Ladam[4] and F. Vittoz[4]

The potential of cryogenic helium flows for studying high-Reynolds number turbulence in the laboratory has been recognised for a long time and implemented in several small-scale hydrodynamic experiments. With its large superconducting particle accelerators and detector magnets, CERN, the European Laboratory for Particle Physics, has become a major world center in helium cryogenics, with several large helium refrigerators having capacities up to 18 kW @ 4.5 K.

Combining a small fraction of these resources with the expertise of three laboratories at the forefront of turbulence research, has led to the design, swift implementation, and successful operation of GReC (Grands Reynolds Cryogéniques) a large axisymmetric turbulent-jet experiment. With flow-rates up to 260 g/s of gaseous helium at $\approx$ 5 K and atmospheric pressure, Reynolds numbers up to $10^7$ have been achieved in a 4.6 m high, 1.4 m diameter cryostat. This paper presents the results of the first runs and describes the experimental set-up comprehensively equipped with "hot" wire micro-anemometers, acoustic scattering vorticity measurements and a large-bandwidth data acquisition system.

1 CERN, LHC Division
2 Centre de Recherches sur les Très Basses Températures (CRTBT), UJF-INPG-CNRS, Grenoble, France
3 Laboratoire des Ecoulements Géophysiques et Industriels (LEGI - IMG), UJF-INPG-CNRS, Grenoble, France
4 Ecole Normale Supérieure (ENSL), Physics Department, Lyon France

# A CRYOGENIC HIGH-REYNOLDS
# TURBULENCE EXPERIMENT AT CERN

A. Bézaguet[1], J.-P. Dauvergne[1], S. Knoops[1], P. Lebrun[1], M. Pezzetti[1],
O. Pirotte[1], J.-L. Bret[2], B. Chabaud[2], G. Garde[2], C. Guttin[2], B. Hébral[2],
S. Pietropinto[2], P. Roche[2], J.-P. Barbier-Neyret[3], C. Baudet[3], Y. Gagne[3],
C. Poulain[3], B. Castaing[4], Y. Ladam[4], F. Vittoz[4]

[1]European Organization for Nuclear Research - CERN
1211 Geneva-23, Switzerland

[2]Centre de Recherches sur les Très Basses Températures (CRTBT)
UJF - INPG - CNRS
B.P. 166, 38042 Grenoble Cedex 9, France

[3]Laboratoire des Ecoulements Géophysiques et Industriels (LEGI - IMG)
UJF - INPG - CNRS
B.P. 53, 38041 Grenoble Cedex 9, France

[4]Ecole Normale Supérieure (ENSL)
Physics Department
46 Allée d'Italie, 69364 Lyon Cedex 7, France

**ABSTRACT**

The potential of cryogenic helium flows for studying high-Reynolds number turbulence in the laboratory has been recognised for a long time and implemented in several small-scale hydrodynamic experiments. With its large superconducting particle accelerators and detector magnets, CERN, the European Laboratory for Particle Physics, has become a major world center in helium cryogenics, with several large helium refrigerators having capacities up to 18 kW @ 4.5 K.

Combining a small fraction of these resources with the expertise of three laboratories at the forefront of turbulence research, has led to the design, swift implementation, and successful operation of GReC (Grands Reynolds Cryogéniques) a large axisymmetric turbulent-jet experiment. With flow-rates up to 260 g/s of gaseous helium at $\approx 5$ K and atmospheric pressure, Reynolds numbers up to $10^7$ have been achieved in a 4.6 m high, 1.4 m diameter cryostat. This paper presents the results of the first runs and describes the experimental set-up comprehensively equipped with "hot" wire micro-anemometers, acoustic scattering vorticity measurements and a large-bandwidth data acquisition system.

## INTRODUCTION

We developed a cryogenic turbulence experiment, that reaches the highest Reynolds number flows ever attained within laboratory conditions. The goal is to investigate turbulence close to the so-called ultimate regime, and to characterize small-scale intermittency of the local velocity field. Two kind of measurements have been performed : on one hand, we used home-made cryogenic "hot" wires to measure the local turbulent velocity fluctuations on the jet axis. On the other hand, we performed spectral measurements of the turbulent vorticity field, resorting to an ultra-sonic scattering method.

This experiment is hosted in CERN, the European Laboratory for Particle Physics, which is also a major world center in helium cryogenics. This project was conducted within a collaboration gathering the Centre de Recherches sur les Très Basses Températures (CRTBT - Grenoble), the Laboratoire des Ecoulements Géophysiques et Industriels (LEGI - Grenoble) and the Physics Department of Ecole Normale Supérieure (ENS - Lyon).

## CRYOGENIC SET-UP

CERN hosted the GReC experiment in the cryogenic test-area devoted to LHC component tests. The test programme showed that it is possible to share the use of the 6kW @ 4.5K cryoplant normally dedicated to the tests of the magnet string representing a full cell of the LHC lattice [1]. Moreover the GReC test set-up (Fig. 1) could be built with a removable transfer line between the refrigerator and the experiment, so that only a half day was necessary to swap between the GReC experiment and the magnet string test facility. To house the experiment, CERN recycled a cryostat which was previously used to test the LEP superconducting acceleration cavities.

To reach the highest possible Reynolds number and to measure it accurately, GReC requested that the facility be run with the coldest possible gas, without any liquid droplets, and the maximum flow rate with the most stable steady-state conditions. Considering the operating mode of this refrigerator, the requested gas flow stability could only be achieved by keeping the refrigerator with a fixed reference point, i.e. a constant level of LHe in the
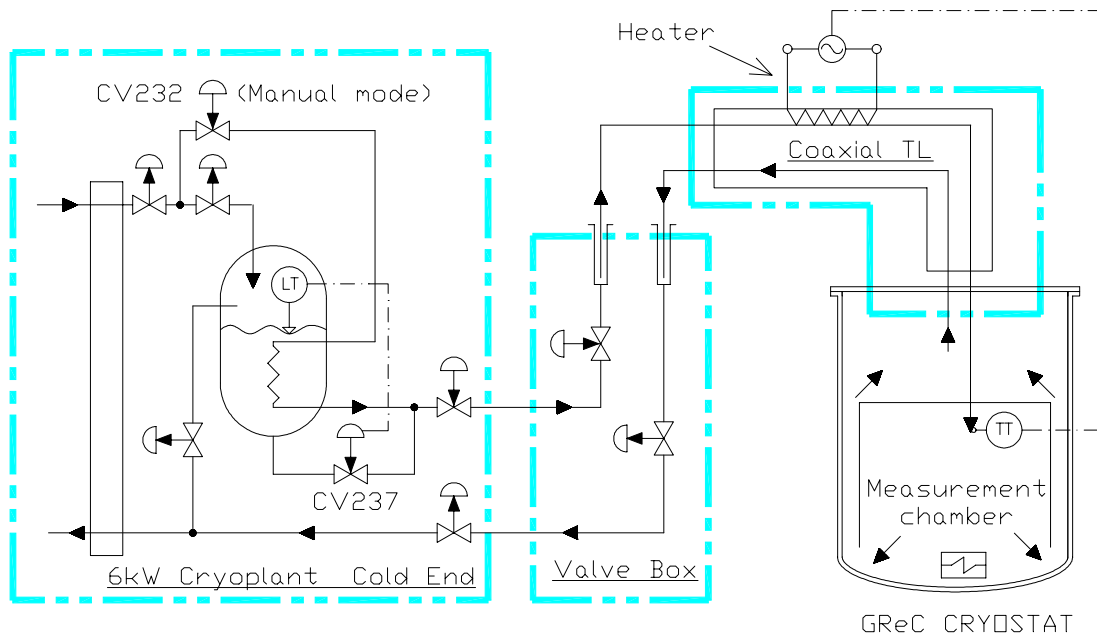


**FIGURE 1.** Cryogenic flow scheme for the GReC experiment and main control parameters.

phase separator. To feed the test cryostat, a coaxial transfer line (6 m long) including a 6 kW controlled heater was developed and installed. The coaxial transfer line was constructed without the usual vacuum separating the inlet and return lines. In this way, it performs as a distributed heat exchanger : the liquid helium is fully vaporized and its temperature homogenized.

To cope with this "exotic" mode of operation, the control system of the test set-up has been integrated into that of the refrigerator. The cold box phase separator level was maintained constant with the valve CV237 (see Fig. 1) normally supplying saturated liquid. In order to attain the best flow stability, the flow rate was adjusted by manual control of valve CV232, normally supplying supercritical helium at 4.5 K. The temperature at the inlet of the jet was controlled by a feedback loop with the heater inside the transfer line.

## THE EXPERIMENT

The flow is an axisymmetrical round jet, developing in a 1 m diameter, 2.5 m high chamber (the cryostat is 1.4 m outer diameter, and 4.6 m high : see Fig. 2). The jet develops downstream from a conical nozzle with 100:1 surface contraction ratio (the nozzle diameter is 25 mm). The cryogenic set-up facility provides a steady gaseous helium jet with flow rates up to 260 g/s, at 4.8 K at atmospheric pressure. These characteristics correspond to Reynolds numbers as high as $10^7$ (i.e. a Taylor-scale based Reynolds number about $R_\lambda \approx 6100$). For comparison, an industrial wind tunnel can reach $R_\lambda \approx 3000$ [2], and geophysical turbulence (ocean or atmosphere) may be roughly estimated to $R_\lambda \approx 8000$ to 10000 (though in less stationary conditions).
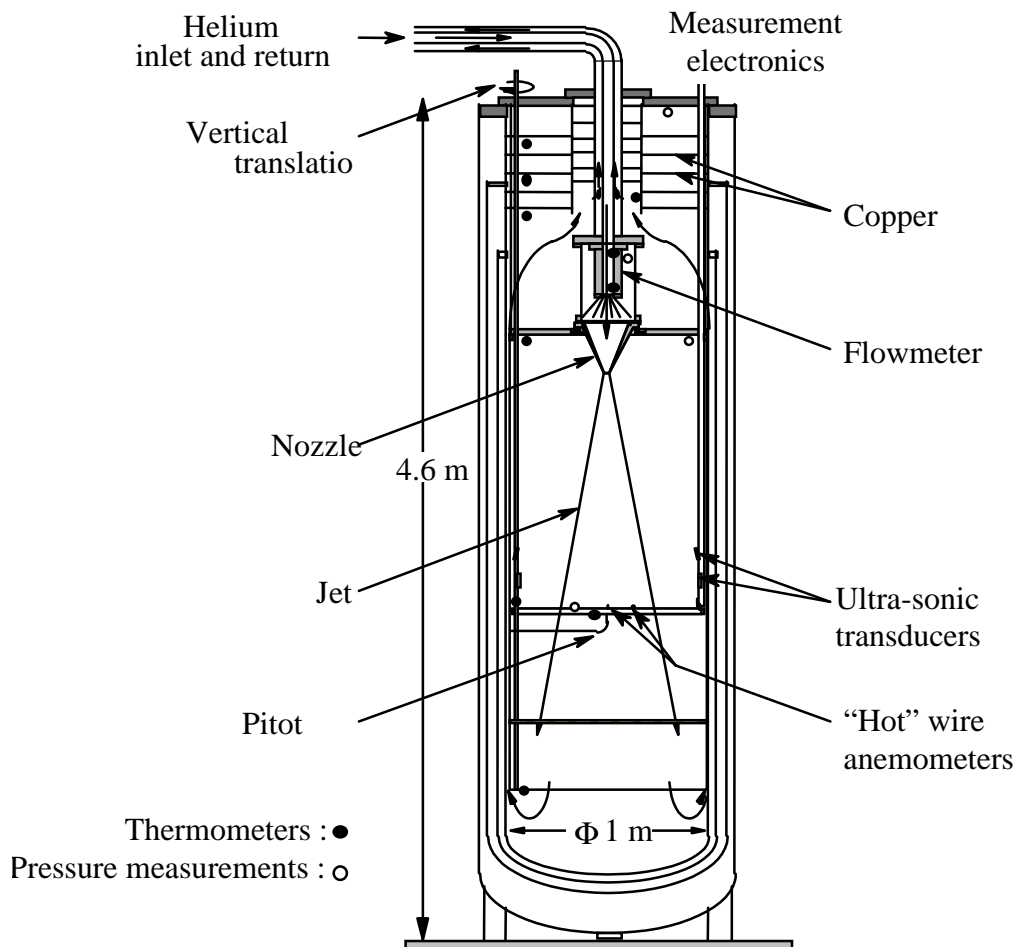


**FIGURE 2.** The GReC cryostat, with temperature and pressure measurement locations.

**TABLE 1.** Main flow characteristics for a few experimental data.

| Mass flow (g/s) | $u_{nozzle}$ (m/s) | $u_{average}$ (m/s) | u' (m/s) | $Re_{nozzle}$ ($10^7$) | $R_\lambda$ |
|---|---|---|---|---|---|
| 20 | 2.5 | 0.3 | 0.08 | 0.077 | 1750 |
| 80 | 9.8 | 1.2 | 0.42 | 0.31 | 3500 |
| 260 | 32.3 | 3.9 | 1.5 | 1.01 | 6100 |

Local velocity measurements are performed at 50 nozzle diameters downstream from the nozzle ($\approx$ 125 cm). At this distance, turbulence is fully developed [3]. The values of the average and standard deviation velocity (measured with a Pitot tube with fast enough response time) are in good agreement with results previously obtained both in a classical air round jet [3] and in a smaller low-temperature helium jet [4, 5].

Table 1 gives a representative set of experimental conditions we have investigated. $u_{nozzle}$ and $u_{average}$ are respectively the nozzle velocity and the average velocity at the measurement location for the turbulence field, u' is the standard deviation of the streamwise component of the velocity fluctuations. The Taylor Reynolds number $R_\lambda$, characteristic of inertial scales, is consistent with the empirical formula proposed by Antonia et al. [6].

## JET AND CONTROL PARAMETERS

The Reynolds number depends on the mass flow rate, and on the fluid viscosity, that varies with temperature and pressure. These latter parameters have thus to be well controled and precisely measured.

The pressure is recorded with a commercial gauge operating at room temperature. In order to estimate the temperature stability along the flow, temperature is measured at various locations in the experiment. Platinum sensors are used to monitor temperature during the cool down to 50 K. At the working temperature (around 5 K), we use calibrated germanium thermometers. A cryogenic resistance bridge with $10^{-4}$ relative resolution allows the temperature to be measured with an absolute precision better than 5 mK. The analog signal (between 0 and 1 V) from the chamber thermometer, is sent back to the liquefier control room, where it is used as the main signal for flow regulation. In steady-state conditions, temperature and pressure stability are better than 1 % (see Fig. 3).
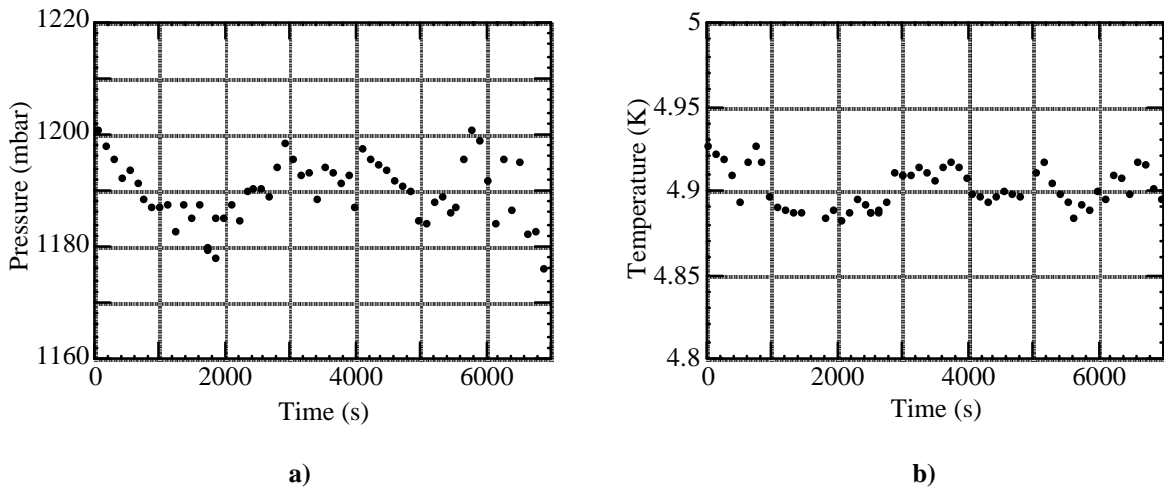


**FIGURE 3. a)** Pressure (1190 ± 12 mbar) and **b)** Temperature (4.90 ± 0.03 K) records during a ≈ 2 hours period for a 250 g/s gaseous helium flow.
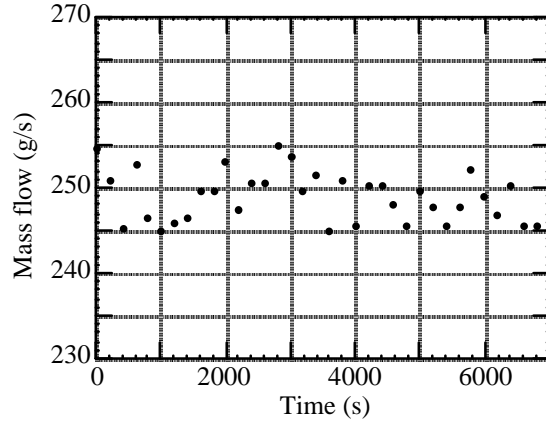
**FIGURE 4.** Mass flow (250 ± 5 g/s) records during a ≈ 2 hours period.

Helium flow rate is derived from the pressure drop across the conical nozzle, using a differential pressure gauge. Figure 4 shows a mass flow record during a 2 hours period, at 250 g/s gaseous helium flow. Mass flow stability is better than 2 %.

## LOCAL VELOCITY MEASUREMENTS

We performed local velocity fluctuations measurements on the jet axis, with home-made "hot" wire anemometers [7]. The sensor is made of a 2 to 5 µm diameter glass fiber coated with a 400 Å Cr + Au layer. This resistive layer is covered by a 2000 Å thick superconducting PbIn alloy, except on a short central length (2 to 5 µm) which acts as the sensitive area (see Fig 5). When heated by the Joule effect, the bare Cr + Au spot induces a transition of the adjacent superconducting alloy. The normal state PbIn length - and thus the global resistance - varies with the local flow velocity.

Specific measurement electronics have been developed : the sensor is one branch of a bridge which is fed by a 10 MHz current. A lock-in amplifier and a PID regulator adjust the current amplitude in the sensor to hold it at a constant resistance [8]. The response time of the whole regulation loop is better than 5 µs, leading to a spatial resolution of about 10 µm that is necessary to study the whole inertial range of length scales.

The raw voltage signal obtained from the "hot" wire electronics is converted into a velocity signal : we assume that the turbulent velocity statistical distribution is marginally gaussian. Its average and standard deviation values being determined from independant measurements (mass flow rate, acoustic scattering), we infer the experimental calibration law.
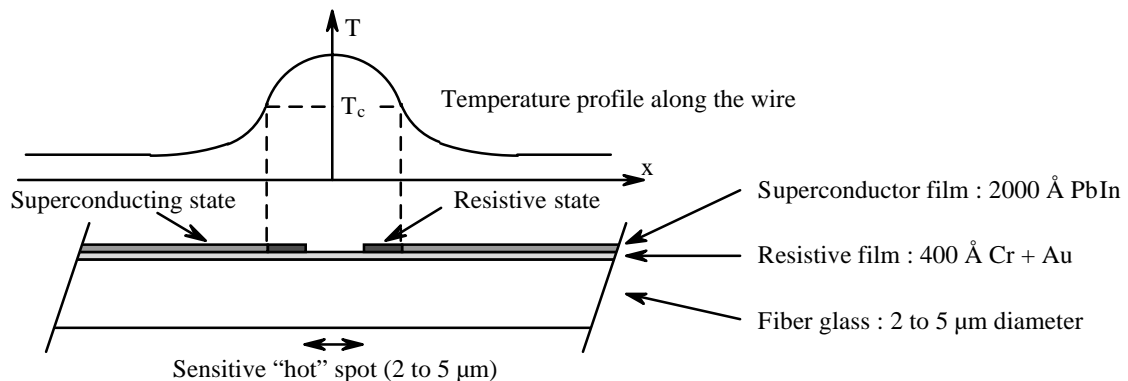


**FIGURE 5.** Cross section of the cryogenic "hot" wire. Length of normal (resistive) part of Pb In thin film is held constant by the regulation electronics.
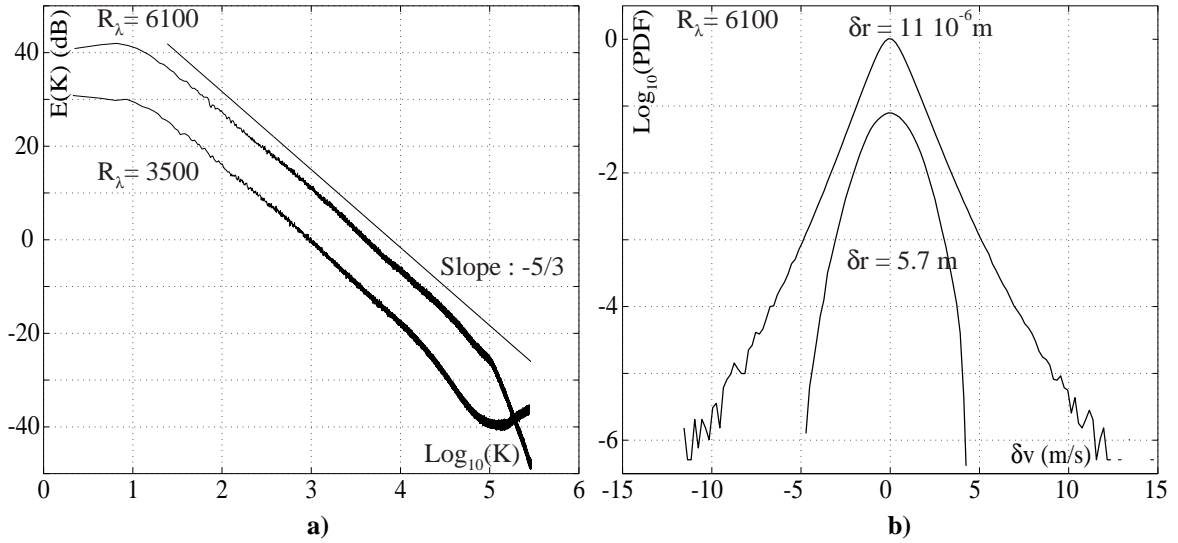
**FIGURE 6. a)** Velocity power spectra, for $R_\lambda = 6100$ and $R_\lambda = 3500$. The straight line with -5/3 slope is given for comparison. K is the wave number ($m^{-1}$)  **b)** Probability density functions of spatial velocity increments ($R_\lambda = 6100$ ) in semilog coordinates. The plot for $\delta r = 5.7$ µm has been shifted a decade down for figure clarity.

Time velocity signals are then converted into spatial velocity fluctuations, assuming the well-known Taylor frozen turbulence hypothesis [9]. Since a large range of scales are involved in the flow, very large continuous data samples have been recorded (typically $10^9$ points, up to 1.2 MHz sampling frequency, for various Reynolds numbers ranging from $7.7 \ 10^5$ to $1.01 \ 10^7$). These data are presently being validated and analysed.

When converted into a local velocity file, the signal can be analysed and transformed by Fourier methods. Figure 6 a) shows spatial velocity spectra obtained for two Reynolds numbers ($R_\lambda = 3500$ and $R_\lambda = 6100$). Spurious frequency lines in the signal have been removed with an appropriate technique known as EMD (Empirical Mode Decomposition [10]). These plots are a straight line in a log-log representation, over a very large range of inertial scales. To our knowledge, it is the first time an inertial power law extending over such a wide range of length scales (up to four decades), has been measured in a laboratory flow. The main result is that this inertial slope is very close to the -5/3 value, in accordance with Kolmogorov's theory of 1941. As expected, such spectra cannot reveal intermittency effects. The experimental data at high frequency are not reliable enough to probe the dissipative viscous scales.

Figure 6 b) displays the Probability Density Functions (PDF) of spatial velocity increments, defined as $\delta u(r) = u(r+\delta r) - u(r)$, for two scales $\delta r$ corresponding to the largest and smallest scales of the inertial range. These PDFs are in agreement with all those previously published [4]. Our data confirm that velocity distribution is quasi-gaussian at large scales (of the order of the integral scale) and on the other side, presents exponential-like tails at small scales. This fact, which characterizes high-Reynolds turbulent flows, is the signature of small-scale intermittency. This is the main property (up to now, not understood) of the so-called fully developed turbulence.

## ACOUSTIC SCATTERING

Acoustic scattering of coherent ultrasonic waves has been successfully used to directly measure the spatial distribution of the turbulent vorticity field. The vorticity field $\mathbf{\Omega}(\mathbf{r},t) = \nabla \times \mathbf{u}(\mathbf{r},t)$ is usually defined as the curl of the local velocity field. The amplitude of vector $\mathbf{\Omega}(\mathbf{r},t)$ is a measurement of the local angular velocity of the fluid elements, while its orientation indicates the direction of the instantaneous rotation axis. In addition, as in any scattering process, the scattered acoustic pressure amplitude is linearly related to $\mathbf{\Omega}(\mathbf{q}_{scatt},t)$,

the spatial Fourier transform at the spatial wavevector $\mathbf{q_{scatt}}$. The ratio of the scattered to the incident acoustic amplitudes may be written [11-14] :

$$\frac{p_{scatt}(\omega)}{p_{inc}(\omega_o)} = \pi^2 i \frac{-\cos(\theta_{scatt})}{1-\cos(\theta_{scatt})} \frac{ve^{i\omega D/c}}{c^2 D} (\mathbf{n} \times \mathbf{r}) \cdot \tilde{\Omega}(\mathbf{q_{scatt}}, \omega - \omega_o) \qquad (1)$$

where $\mathbf{n}$ and $\mathbf{r}$ are the unitary vectors in the incident and scattered directions.

The acoustic waves are produced and detected by means of electroacoustic reversible tranducers of Sell type (circular), operated at about 5 K. Their size (5 cm diameter), location and relative arrangement is such that the measurement volume is on the jet axis, close to the "hot" wire anemometers (50 nozzle diameter downstream). In the present experiment, the scattering wavevector $\mathbf{q_{scatt}}$, defining the characteristics of the band-pass spatial filtering is adjusted by tuning the frequency $\omega_0$ of the incident acoustic wave (between 30 kHz and 230 kHz). The scattering angle $\theta_{scatt}$ remains constant and equal to 30° :

$$\mathbf{q_{scatt}} \cong 2\frac{\omega_o}{c}\sin\left(\frac{\theta_{scatt}}{2}\right)\frac{\mathbf{n}-\mathbf{r}}{|\mathbf{n}-\mathbf{r}|} \qquad (2)$$

In our experimental conditions, the helium sound velocity is close to 130 m/s, and the incident acoustic frequencies and scattering angle allow the analysis of length scales in the inertial range.

In the present context, acoustic scattering by the vorticity enables the continuous probing in real time of coherent vorticity structures, which form in the flow as a result of the turbulent cascade process. These vorticity structures are known to be advected by the large scale velocity flow (Kelvin theorem) and can thus serve as velocity marker. The advection of the scatterers present at some time in the measurement volume results in a Doppler shift $\Delta v$ of the scattered acoustic wave frequency, with respect to the incident monochromatic wave : $2\pi\Delta v = \omega - \omega_0 = \mathbf{q_{scatt}} \cdot \mathbf{u}$.

Thanks to the transducers linearity, and using numerical heterodyne detection, we are able to resolve the small and fluctuating Doppler frequency shifts (less than 1 kHz), appearing as nonsymmetrical (with respect to the incoming frequency) time spectra of the scattered pressure signals. Several acoustic measurements have been performed, at the same scattering angle, for different incoming sound frequencies $v_0$, ranging from 30 kHz to 230 kHz. Three acoustic scattering spectra, corresponding to three different wavevectors
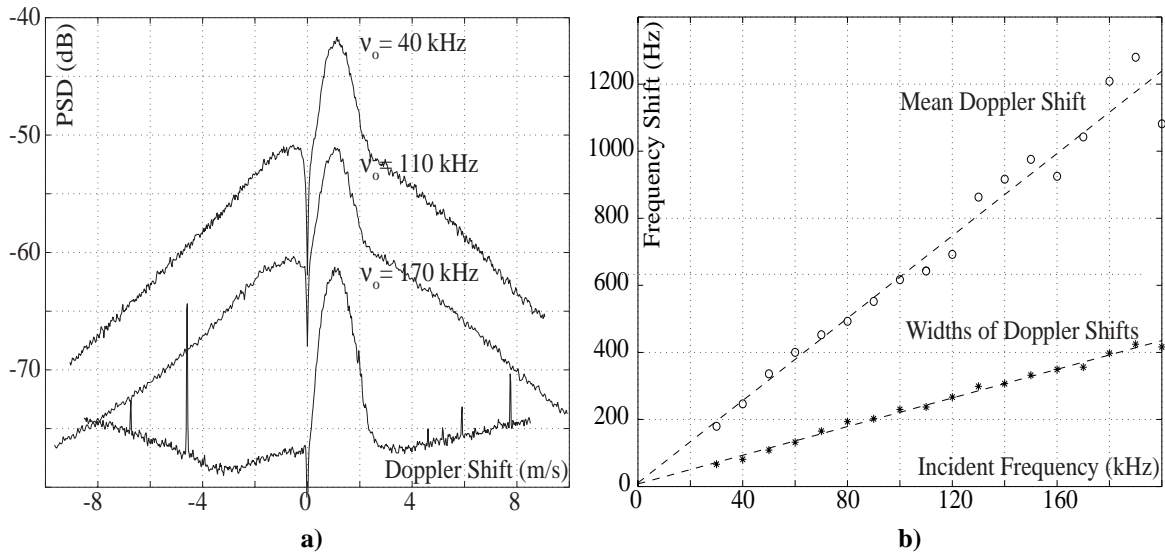


**FIGURE 7. a)** Spectra of the scattered acoustic pressure for three incident wave frequencies (40 kHz, 110 kHz and 170 kHz), at $R_\lambda = 3500$. **b)** Linear evolution of the mean and width of the Doppler peak as a function of the incoming sound frequency at $R_\lambda = 3500$.

$q_{scatt}$, are plotted in figure 7 a), as a function of the Doppler shift expressed in m/s according to $|\mathbf{u}| = 2\pi \Delta v/|\mathbf{q_{scatt}}|$. Around the expected mean Doppler shift (related to the average flow velocity), we observe a wide Doppler peak with a gaussian shape, in agreement with the expected statistics of the large-scale flow velocity.

All the spectra lead to close estimations of the average (position of the maximum) and the standard deviation (related to the Doppler peak width) of the flow velocity. This latter fact is illustrated in figure 7 b), where we have plotted the evolution of the mean value and width of the Doppler shifts as a function of the incoming sound frequencies $v_0$. The linear behaviour of both quantities is an experimental confirmation of the validity of the Taylor hypothesis. Performing a linear fit to estimate the slopes of these two curves, gives another estimation of the values of average and standard deviation of the velocity, in agreement with the other measurements (Pitot tube and mass flow rate).

## OUTLOOK

We have successfully operated a high-Reynolds low temperature helium jet. This flow has been extensively tested and its hydrodynamic characteristics are in agreement with those of classical jets. Controlled and reproducible conditions are available and allow us to reach the highest laboratory Reynolds numbers. This experiment constitutes a first step towards the possible development of large-scale cryogenic turbulence facilities.

## ACKNOWLEDGEMENTS

## REFERENCES

1. Erdt, W.K., Frandsen, P., Güsewell, D., Solheim, N.O., Winkler, G., Kurtcuoglu, K., Löhlein, K., Senn, A.E., Wagner, U. and Ziegler, B., *Adv. Cryog. Eng.*, **39A**, 553 (1994).
2. Gagne, Y., Hopfinger, E. and Frisch, U., *NewTrends in Nonlinear Dynamics and Pattern Forming Phenomena*, NATO - ASI Plenum Press, New-York, **237**, 315 (1990).
3. Wygnanski, I. and Fiedler, H., *J. Fluid Mech.*, **38**, 577 (1969).
4. Chabaud, B., Naert, A., Peinke, J., Chillà, F., Castaing, B. and Hébral, B., *Phys. Rev. Lett.*, **73**, 3227 (1994).
5. Chanal, O., Chabaud, B., Castaing, B. and Hébral, B., *Eur. Phys. J. B*, **17**, 309 (2000).
6. Antonia, R.A., Satyaprakash, B.R. and Hussain, A.K.M., *Phys. Fluid*, **23**, 695 (1980).
7. Castaing, B., Chabaud, B. and Hébral, B., *Rev. Sci. Inst.*, **63**, 4167 (1992).
8. Bret, J.-L. and Guttin, C., *Internal report*, CNRS – CRTBT, Grenoble (2000).
9. Kahalerras, H., Malécot, Y., Gagne, Y. and Castaing, B., *Phys. Fluid*, **10**, 910 (1998).
10. Huang, N.E., Shen, Z., Long, S.R., Wu, M.C., Shih, H.H., Zheng, Q., Yen, N.-C., Tung, C.C. and Liu, H.H., *Proc. Math. Phys. Eng. Sciences*, **454**, 903 (1998).
11. Kraichnan, R.H., *J. Acoust. Soc. Am.*, **A18**, 6 (1953).
12. Chu, B.T. and Kovàsznay, L.S.G., *J. Fluid Mech.*, **A3**, 494 (1958).
13. Lund, F. and Rojas, C., *Physica D*, **A37** (1989).
14. Baudet, C., Michel, O. and Williams, W.J., *Physica D*, **128**, 1 (1999).